Parkinsonism and Related Disorders 82 (2021) 16–23

Contents lists available at ScienceDirect

Parkinsonism and Related Disorders

journal homepage: www.elsevier.com/locate/parkreldis

Hierarchical cluster analysis of multimodal imaging data identifies brain atrophy and cognitive patterns in Parkinson's disease

A. Inguanzo [a,b,c], R. Sala-Llonch [a,c,d,e], B. Segura [a,b,c,f,*], H. Erostarbe [a], A. Abos [a,b,c], A. Campabadal [a,b,c], C. Uribe [a,b], H.C. Baggio [a,b], Y. Compta [a,c,f,g], M.J. Marti [a,c,f,g], F. Valldeoriola [a,c,f,g], N. Bargallo [h,i], C. Junque [a,b,c,f]

[a] Institute of Neurosciences, University of Barcelona, Barcelona, Catalonia, Spain
[b] Medical Psychology Unit, Department of Medicine, University of Barcelona, Barcelona, Catalonia, Spain
[c] Institute of Biomedical Research August Pi i Sunyer (IDIBAPS), Barcelona, Catalonia, Spain
[d] Department of Biomedicine, University of Barcelona, Barcelona, Catalonia, Spain
[e] Centro de Investigación Biomédica en Red en Bioingeniería, Biomateriales y Nanomedicina (CIBER-BBN), Barcelona, Catalonia, Spain
[f] Centro de Investigación Biomédica en Red Sobre Enfermedades Neurodegenerativas (CIBERNED: CB06/05/0018-ISCIII), Barcelona, Catalonia, Spain
[g] Movement Disorders Unit, Neurology Service, Hospital Clínic de Barcelona, University of Barcelona, Barcelona, Catalonia, Spain
[h] Centre de Diagnostic per la imatge, Hospital Clínic de Barcelona, Barcelona, Catalonia, Spain
[i] Magnetic Resonance Core Facility, Institute of Biomedical Research August Pi i Sunyer (IDIBAPS). Barcelona, Catalonia, Spain

ARTICLE INFO

Keywords:
Parkinson disease
Cluster analysis
Magnetic resonance imaging
DTI
Gray matter volume

ABSTRACT

Background: Parkinson's disease (PD) is a heterogeneous condition. Cluster analysis based on cortical thickness has been used to define distinct patterns of brain atrophy in PD. However, the potential of other neuroimaging modalities, such as white matter (WM) fractional anisotropy (FA), which has also been demonstrated to be altered in PD, has not been investigated.

Objective: We aim to characterize PD subtypes using a multimodal clustering approach based on cortical and subcortical gray matter (GM) volumes and FA measures.

Methods: We included T1-weighted and diffusion-weighted MRI data from 62 PD patients and 33 healthy controls. We extracted mean GM volumes from 48 cortical and 17 subcortical regions using FSL-VBM, and the mean FA from 20 WM tracts using Tract-Based Spatial Statistics (TBSS). Hierarchical cluster analysis was performed with the PD sample using Ward's linkage method. Whole-brain voxel-wise intergroup comparisons of VBM and TBSS data were also performed using FSL. Neuropsychological and demographic statistical analyses were conducted using IBM SPSS Statistics 25.0.

Results: We identified three PD subtypes, with prominent differences in GM patterns and little WM involvement. One group (n = 15) with widespread cortical and subcortical GM volume and WM FA reductions and pronounced cognitive deficits; a second group (n = 21) with only cortical atrophy limited to frontal and temporal regions and more specific neuropsychological impairment, and a third group (n = 26) without detectable atrophy or cognition impairment.

Conclusion: Multimodal MRI data allows classifying PD patients into groups according to GM and WM patterns, which in turn are associated with the cognitive profile.

1. Introduction

Parkinson's disease (PD) is characterized by its clinical heterogeneity, which includes not only motor symptoms but also a wide range of non-motor manifestations [1,2]. Objective neuroimaging data obtained from magnetic resonance imaging (MRI) has been

* Corresponding author. Medical Psychology Unit, Department of Medicine, University of Barcelona, Casanova 143, 08036, Barcelona, Spain.
E-mail addresses: annainguanzo@ub.edu (A. Inguanzo), roser.sala@ub.edu (R. Sala-Llonch), bsegura@ub.edu (B. Segura), herostga7@alumnes.ub.edu (H. Erostarbe), alexandraabos@ub.edu (A. Abos), anna.campabadal@ub.edu (A. Campabadal), carme.uribe@ub.edu (C. Uribe), hbaggio@ub.edu (H.C. Baggio), ycompta@clinic.cat (Y. Compta), mjmarti@clinic.cat (M.J. Marti), fvallde@clinic.cat (F. Valldeoriola), bargallo@clinic.cat (N. Bargallo), cjunque@ub.edu (C. Junque).

https://doi.org/10.1016/j.parkreldis.2020.11.010
Received 17 January 2020; Received in revised form 15 September 2020; Accepted 10 November 2020
Available online 12 November 2020

demonstrated to be able to classify PD patients through cluster analysis. Uribe et al. [3] used cortical thickness from MRI data to define distinct anatomical subtypes in a non-demented PD sample, and found one group with frontal and occipital atrophy, a second group with parieto-temporal atrophy and a third with undetectable atrophy. These three patterns were then found to be associated with different clinical/cognitive profiles. Moreover, a follow up of this study concluded that the three patterns progressed differently over time, the pattern with the youngest age at onset being the one associated with the least structural degeneration [4].

These studies have used cortical thickness to define the clusters representing atrophy profiles. However, previous studies have also shown volumetric differences in cortical and subcortical GM regions [5] as well as microstructural white matter (WM) alterations in PD [6]. In addition, GM and WM changes have been widely shown to be associated with cognitive impairment [5,7–9]. Recently, disruption of integration of structural brain networks was observed in PD subtypes identified through clinical data and was correlated with motor and cognitive deficits [10].

To date, no previous studies have combined GM and WM information extracted from MRI to detect different disease subgroups in PD using a multimodal hypothesis-free data-driven approach. We hypothesized that multimodal clustering including FA measures would allow us to more accurately identify subgroups of patients characterized by different patterns of neurodegeneration, which at the same time would be associated with distinctive clinical and neuropsychological phenotypes. Accordingly, we aimed to combine measures of GM cortical and subcortical volumes, as well as measures of WM microstructure to determine (1) whether different anatomical profiles exist involving GM and WM patterns of brain atrophy; and (2) whether the different patterns are associated with distinct cognitive profiles.

2. Methods

2.1. Participants

The sample included 69 PD patients recruited from the Parkinson's Disease and Movement Disorders Unit, Hospital Clínic (Barcelona, Spain), and 36 healthy controls (HC) from the Aging Institute in Barcelona. Inclusion criteria for patients were (i) fulfilling UK PD Society Brain Bank diagnostic criteria for PD and (ii) no surgical treatment with deep-brain stimulation. Exclusion criteria for all participants were (i) dementia according to Movement Disorders Society criteria, (ii) Hoehn and Yahr (H&Y) scale score > 3, (iii) severe psychiatric or neurological comorbidity, (iv) low global intelligence quotient estimated by the Vocabulary subtest of the Wechsler Adult Intelligence Scale 3rd edition (scalar score ≤ 7), (v) Mini Mental State Examination (MMSE) score below 25, (vi) claustrophobia, (vii) pathological MRI findings other than mild WM hyperintensities in the FLAIR sequence, and (viii) MRI artifacts. A total of 62 PD patients and 33 HC were selected. The following participants were excluded from the study: five patients and two HC with MRI artifacts, two patients with claustrophobia and one HC with a cyst. The final sample included participants with and without mild cognitive impairment (MCI). Motor symptoms were assessed with the Unified Parkinson's Disease Rating Scale, motor section (UPDRS-III). All PD patients were taking antiparkinsonian drugs that consisted of different combinations of L-dopa, catechol-O-methyltransferase inhibitors, monoamine oxidase inhibitors, dopamine agonists, and amantadine. To standardize the doses, the L-dopa equivalent daily dose (LEDD) [11] was calculated. Written informed consent was obtained from all study participants after a full explanation of the procedures. The study was approved by the institutional Ethics Committee from the University of Barcelona (IRB00003099).

2.2. Neuropsychological tests

All participants underwent a comprehensive neuropsychological assessment in the *on state* addressing cognitive domains frequently impaired in PD [12]. Attention and working memory were assessed with the Trail Making Test (parts A and B), Digit Span Forward and Backward, Stroop Color-word Test, Symbol Digits Modalities Test (SDMT)-Oral version. Executive functions were evaluated with phonemic and semantic fluencies. Language was assessed using the Boston Naming Test (BNT). Memory was assessed using Rey's Auditory Verbal Learning Test total learning recall, delayed recall and recognition abilities (RAVLT total, RAVLT recall, and RAVLT recognition, respectively). Visuospatial and visuoperceptual functions were assessed with Benton's Judgement of Line Orientation (JLO), Visual Form Discrimination (VFD), and Facial Recognition (FRT) tests. Neuropsychiatric symptoms were evaluated with the Beck Depression Inventory-II, Starkstein's Apathy Scale and Cumming's Neuropsychiatric Inventory. Expected z scores adjusted for age, sex, and education were calculated for each test and subject based on a multiple regression analysis performed in the HC group [13]. The presence of MCI was defined using PD-MCI diagnostic criteria level I [12].

2.3. Neuroimaging data

2.3.1. MRI acquisition

MRI data were obtained with a 3T scanner (MAGNETOM Trio, Siemens, Germany). The scanning protocol included high-resolution 3-dimensional T1-weighted images acquired in the sagittal plane (TR: 2300 ms, TE: 2.98 ms, TI: 900 ms, 240 slices, FOV: 256 mm; 1 mm isotropic voxel), and diffusion-weighted images (DTI): two sets of single band spin-echo diffusion weighted images in the axial plane with opposite (anterior-posterior and posterior-anterior) phase encoding directions (TR: 7700 ms, TE: 89 ms, FOV: 244 mm; 2 mm isotropic voxel; number of directions: 30, b-value: 1000 s/mm^2, b0 value: 0 s/mm^2).

2.3.2. Structural MRI preprocessing

Structural data were analyzed with FSL-VBM [14]. First, structural images were brain-extracted and segmented into GM, WM and cerebrospinal fluid, then registered to the Montreal Neurological Institute (MNI) 152 standard space using non-linear registration. The resulting images were averaged to create a study-specific template, to which native GM images were nonlinearly re-registered. Second, native GM images were registered to this study specific template and modulated to correct for local expansion or contraction due to the nonlinear component of the spatial transformation. The modulated GM images were then smoothed with an isotropic Gaussian kernel with a sigma of 3 mm (FWHM = 6.9 mm) following the FSL guidelines [14].

2.3.3. Diffusion MRI preprocessing

Diffusion MRI images were analyzed with FMRIB's Diffusion Toolbox (FDT) software from FSL, (http://www.fmrib.ox.ac.uk/fsl). Individual fractional anisotropy (FA) maps were obtained using a Diffusion Tensor Model fit (DTIFIT) and introduced to group analysis using the Tract-Based Spatial Statistics (TBSS) protocol [15,16]. TBSS performs non-linear registration (FNIRT) of FA images to the MNI standard space and generates a mean FA skeleton that represents the center of all tracts common to the entire group. Then, the aligned FA image for each subject was projected onto the skeleton by filling the skeleton with FA values from the nearest relevant tract center.

2.4. Hierarchical cluster analysis

As described above, we obtained individual GM probability maps using a VBM approach and skeletonized FA maps from all subjects using a DTI approach with FSL. Using the FSL command-line fslmeants, we calculated the mean GM volume from 48 cortical regions and 17

subcortical regions of interest defined by the Harvard-Oxford atlases (https://fsl.fmrib.ox.ac.uk/fsl/fslwiki/Atlases) in MNI standard space. Mean FA values were extracted from 20 tracts of interest defined in the JHU atlas [17], also in the MNI standard space. The 85 resulting features were then merged into a single vector for each of the 62 PD patients subject and used to perform a hierarchical cluster analysis with MATLAB (release 2014b, The MathWorks, Inc., Natick, Massachusetts) (Fig. 1). We used Ward's clustering linkage method to combine pairs of clusters at each step while minimizing the sum of square errors from the cluster mean. Following the hierarchical structure of the analysis, each patient was first placed in his/her own cluster and then progressively clustered with others. Calinski-Harabasz criterion was used to evaluate the optimal number of clusters. Cluster analysis results are shown as a dendrogram with different levels of granularity. For each cluster, we defined a mean cluster vector of 85 features, calculated as the average of all features across the subjects included in the cluster.

2.5. Other statistical analyses

First, to quantify the differences between the groups identified through the clustering procedure, and to define their specific atrophy patterns compared with controls, we performed a set of t-tests using the GM and WM measures used as features. The results were corrected for multiple comparisons using false-discovery rate (FDR) correction across the 85 evaluated features, and the significance level was set at $p < 0.05$. To list the features according to their importance in forming the clusters, we used the F statistics obtained from ANOVAs.

We then performed voxel-wise analyses to obtain maps of GM and WM. For that purpose, we used a permutation-based general linear model (GLM) using the whole-brain VBM and FA maps [18]. In these analyses, we tested for differences between PD groups as well as differences between each group and controls. Age was considered as a covariate in the model. Results were corrected for multiple comparisons across space using family-wise error rate (FWE) correction, with a significance level of $p < 0.05$.

Demographic, neuropsychological, and clinical statistical analyses were conducted using IBM SPSS Statistics 25.0 (IBM Corp., Armonk, New York). To assess differences in demographic, clinical and neuropsychological quantitative variables, Kruskal-Wallis or Mann-Whitney U tests were used. Pearson's chi-squared test was used for categorical variables.

3. Results

The dendrogram resulting from the cluster analysis can be seen in the Supplementary material 1. Both two-cluster and three-cluster solutions had a high variance ratio of the Calinski-Harabasz values. The two-cluster solution (variance ratio: 11.58) identified one group without detectable brain atrophy; and a second group with widespread reduction of cortical and subcortical GM volume, decreased FA, late disease onset and higher prevalence of MCI. Detailed information about the two-cluster solution is shown in Supplementary material 2. The three-cluster solution (variance ratio: 8.59) divided the non-specific atrophy group from the two-cluster solution into two subgroups (Supplementary material 2 and 3). The sample size was too small for higher group solution, and the result would be considered too exploratory.

Ordering the features according to their importance for forming the clusters showed GM features were more relevant than the WM features (Supplementary material 4).

3.1. Whole-brain atrophy patterns in the three-cluster solution

Exploratory whole-brain analyses were first performed without covariates (Supplementary material 5, 6 and 7). Whole-brain analysis of VBM maps considering age in the model showed group 1 (PD1, N: 15) had lower GM volumes than HC mainly in occipital and medial temporal

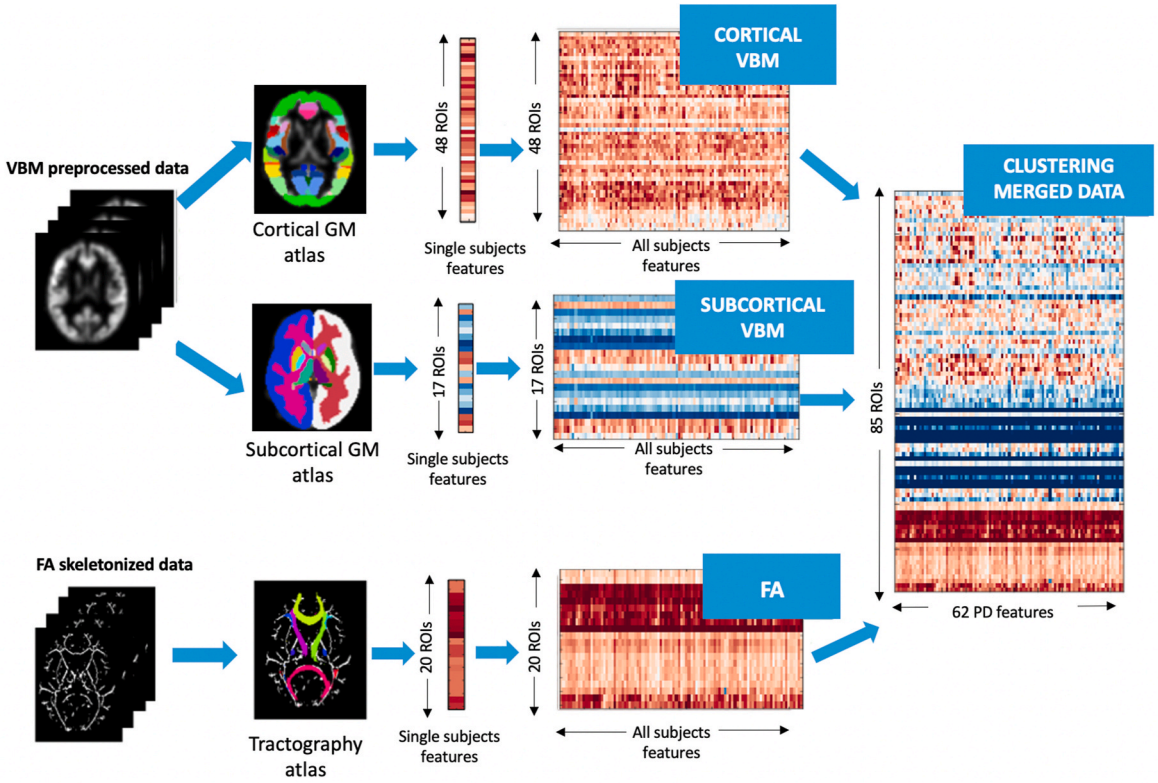

Fig. 1. Schematic representation of the pipeline followed to extract the features used in the classification procedure. Abbreviations: FA – fractional anisotropy, GM – gray matter, ROI – region of interest, VBM – Voxel-based morphometry analysis.

regions including the parahippocampal gyrus, temporal pole, cuneus, lingual gyrus, occipital fusiform gyrus and occipital pole. The atrophy pattern of PD1 also included the bilateral orbital and medial frontal cortex, paracingulate gyrus, superior parietal lobe, precuneus, and insula. Moreover, PD1 showed volume reductions in subcortical gray matter compared to HC in bilateral putamen, caudate, thalamus, and nucleus accumbens as well as the hippocampus (FWE-corrected, $p < 0.05$) (Fig. 2A and Supplementary material 8). Group 2 (PD2, N: 21) had GM atrophy compared with HC mainly in bilateral orbital and prefrontal cortical regions including the bilateral anterior cingulate gyrus, orbitofrontal cortex, medial prefrontal cortex, paracingulate gyri, frontal poles and the inferior and middle temporal gyri, as well as the right superior temporal gyrus (FWE-corrected, $p < 0.05$) (Fig. 2B and Supplementary material 8). Group 3 (PD3, N:26) did not show significant GM volume differences compared with HC (Fig. 2C).

Comparisons between patient groups showed that PD1 had reduced subcortical GM volume compared with PD2 in the thalamus, amygdala and right putamen bilaterally as well as in the hippocampus. PD1 also showed a characteristic posterior cortical atrophy including bilateral occipital poles, lingual gyri and cuneus, together with parahippocampal and fusiform gyri, as well as reductions in insular and cerebellar regions (Supplementary material 8 and 9). PD1 showed reduced cortical GM when compared with PD3 bilaterally in superior and middle temporal gyri, medial temporal lobe, occipital pole, the insular cortex, the

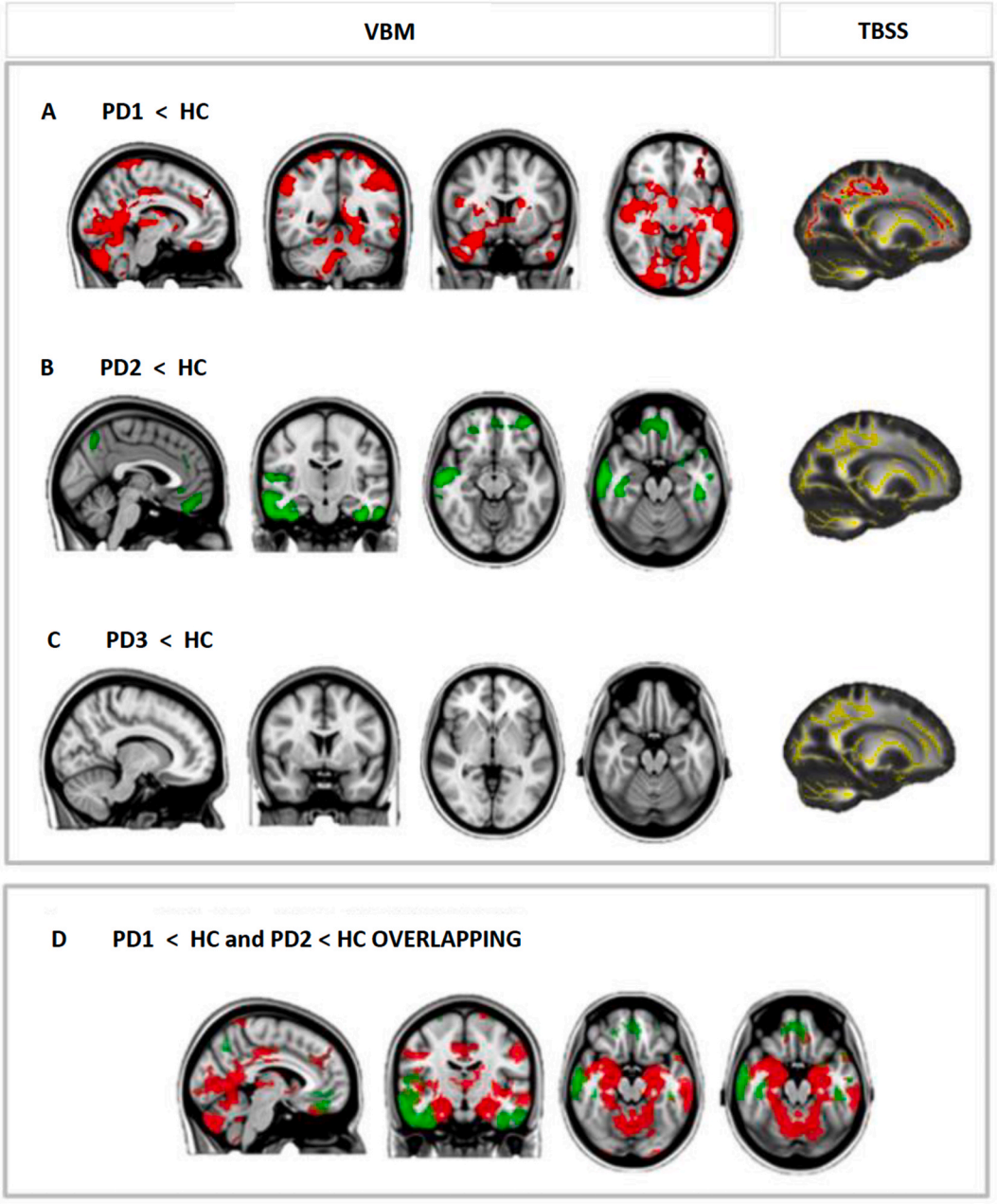

Fig. 2. Voxel-based morphometry (VBM) and tract-based spatial statistics (TBSS) analyses of the three-cluster solution. VBM: (A) regions in which PD1 showed less gray matter volume than HC are shown in red; (B) regions in which PD2 showed less gray matter volume than HC are shown in green; (C) absence of differences between PD3 and HC ($p < 0.05$, FWE-corrected). Results were adjusted by age. TBSS: FA skeleton (yellow) and white matter tracts in which PD1 showed lower FA than HC (red). Radiological convention is used. Abbreviations: HC – healthy controls; PD1 – Parkinson's disease patient subgroup 1; PD2 – Parkinson's disease patient subgroup 2; PD3 – Parkinson's disease patient subgroup 3. (For interpretation of the references to color in this figure legend, the reader is referred to the Web version of this article.)

intracalcarine cortex, and the hippocampus and significant reductions of the amygdala, thalamus, putamen, caudate and nucleus accumbens bilaterally (Supplementary material 8 and 9).

PD2 had less GM volume than PD3 in the right middle temporal gyrus. PD3 had less GM volume than PD2 in the cerebellum and the brainstem. HC had less GM than PD2 in the cerebellum (Supplementary material 8).

Whole-brain analyses of FA maps showed lower FA values in PD1 compared with HC in the corpus callosum and the following bilateral tracts: the inferior and superior longitudinal fasciculus, inferior fronto-occipital fasciculus, anterior thalamic radiation, uncinate fasciculus, corticospinal tract, and forceps major and minor (FWE-corrected, $p < 0.05$) (Fig. 2 and Supplementary material 10). There were no other significant differences between groups.

3.2. Demographic and clinical characteristics of PD subtypes

There were no differences in sex or years of education between groups. However, we did find significant differences in age between groups. PD3 was significantly younger than HC and the other PD groups, while PD1 tended to be older than HC ($p = 0.054$). PD groups did not differ in disease duration, motor disease severity as measured by the UPDRS-III, H&Y and LEDD, global cognition (MMSE), olfactory performance, or presence of neuropsychiatric symptoms. PD1 had a later disease onset compared with PD3 (Table 1).

3.3. Cognitive profiles of PD subtypes

Fig. 3 summarizes the cognitive profiles of patients in the three groups (see also Supplementary Table 11). PD1 and PD2 performed significantly worse than HC in the following tests: FRT, TMT Part A and Part B, and Stroop Color Test. Whereas PD3 did not show significant differences in cognitive performance in comparison with HC.

Moreover, PD1 performed significantly worse than HC and PD3 in RAVLT total and recognition scores, and in the semantic fluency test. PD1 also performed worse than HC in RAVLT recall. PD2 performed worse than HC in Stroop Words and SDMT.

PD1 showed a higher percentage of MCI (67%) when compared with PD3 (27%) and HC (Table 1).

4. Discussion

The main finding of this study is that a data-driven analysis based on multimodal MRI data can identify PD patient subtypes according to GM and WM degeneration patterns. Despite similar disease duration, our results distinguished (1) a group of patients with bilateral tempo-parieto-occipital loss of cortical GM as well as subcortical GM volume degeneration and widespread FA reductions mainly affecting fronto-occipital WM tracts; (2) a second group with reduction of GM volumes in bilateral orbital and medial prefrontal, but also in temporal cortical regions, and (3) a third group without detectable GM or WM alterations.

Patients grouped in PD1, which interestingly was the group with a higher percentage of MCI (67%), showed extensive atrophy similar to that previously reported using cortical thickness [3], as well as evident atrophy in bilateral hippocampus and subcortical structures, including the amygdala, thalamus, putamen and caudate. Similarly, the PD2 subgroup showed bilateral atrophy in orbitofrontal and temporal cortices, which partially overlapped with PD1. In this context, and without longitudinal evidence, these results could be indicative of different stages of evolution in our group. However, PD groups did not differ in the years of evolution of the disease, and although those in PD1 were older than in PD2, age of onset was also older. In addition, there were no differences in UPDRS part III or H&Y scores, or medication. Thus, our results reinforce the classical findings that late onset of the disease is associated with greater degree of atrophy and rapid disease progression [19].

Although most of the published results regarding loss of WM integrity in PD are based on analyses of regions of interest, whole-brain studies evidenced the involvement of the corpus callosum, cingulum and major association tracts in PD-MCI patients [7,9,20], but not in PD without MCI [9]. Nonetheless, these results are still scarce and less consistent than those reporting GM atrophy. In this regard, the existence

Table 1
Demographic and clinical characteristics of the three-cluster solution PD subtypes. Abbreviations: HC – healthy controls; IQ – interquartile range; LEDD – L-dopa equivalent daily dose; MCI – mild cognitive impairment; NA – not applicable; PD1 – Parkinson's disease group 1 patients; PD2 – Parkinson's disease group 2 patients; PD3 – Parkinson's disease group 3 patients; UPDRS – Unified Parkinson's Disease Rating Scale; UPSIT – University of Pennsylvania Smell Identification Test.[a] The chi-squared test was used;[b] The Kruskal-Wallis test was used.

	HC (N:33)	PD1 (N:15)	PD2 (N:21)	PD3 (N:26)	test-stats	p-value	Significant contrasts
sex (m/f)	18/15	13/2	14/7	19/7	5.4	0.145[a]	–
age, median (IQ)	66(15)	75(14)	68(9)	58.5(11)	29.273	<0.001[b]	PD3 vs HC PD3 vs PD2 PD3 vs PD1
Education, years, median (IQ)	12(8)	11(12)	13(9)	13(9)	1.171	0.768[b]	–
Disease duration, median (IQ)	NA	7(7.5)	9(9)	7(5.5)	1.302	0.521[b]	–
Age of onset, median (IQ)	NA	67(10)	57(11)	50(12.25)	20.097	<0.001[b]	PD1 vs PD3
LEDD, mg, median (IQ)	NA	650(415)	469(515)	593.75(324)	0.651	0.722[b]	–
UPDRS part III, median (IQ)	NA	30(1)	29(2)	30(2)	2.258	0.521[b]	–
Hoen & Yahr, n, 1/2/2.5/3	NA	1/6/1/4	1/10/0/9	6/14/0/6	14.754	0.064[a]	–
MMSE, median (IQ)	0.102(3.32)	−0.96(4.32)	0.074(5.58)	−0.51(4.02)	1.908	0.592[b]	–
Total MCI, n (%)	3 (10%)	10 (67%)	10 (48%)	7(27%)	17.431	0.001[a]	PD1 vs HC PD1 vs PD3 PD2 vs HC
UPSIT (normosmia/hyposmia/anosmia)	5/26/0	0/2/12	1/11/8	1/13/11	34.998	<0.001[a]	PD1 vs HC PD2 vs HC PD3 vs HC
Sniffin (normosmia/hyposmia/anosmia)	20/9/0	0/4/7	1/14/3	3/13/6	53.56	<0.001[a]	PD1 vs HC PD2 vs HC PD3 vs HC
BDI, median (IQ)	5(8)	7(10)	9(12)	7(6)	4.5	0.212[b]	–
Apathy scale (apathy/normal)	5/25 (17%)	7/8 (47%)	10/9 (48%)	8/15 (31%)	9.757	0.135[a]	–
NPI, median (IQ)	1(4)	9(8)	7.5(19)	6(11)	19.047	<0.001[b]	PD1 vs HC PD2 vs HC PD3 vs HC
Visual hallucinations (no/yes), n (%)	29/0	11/4 (27%)	18/3 (14%)	21/5 (19%)	7.414	0.06[a]	–

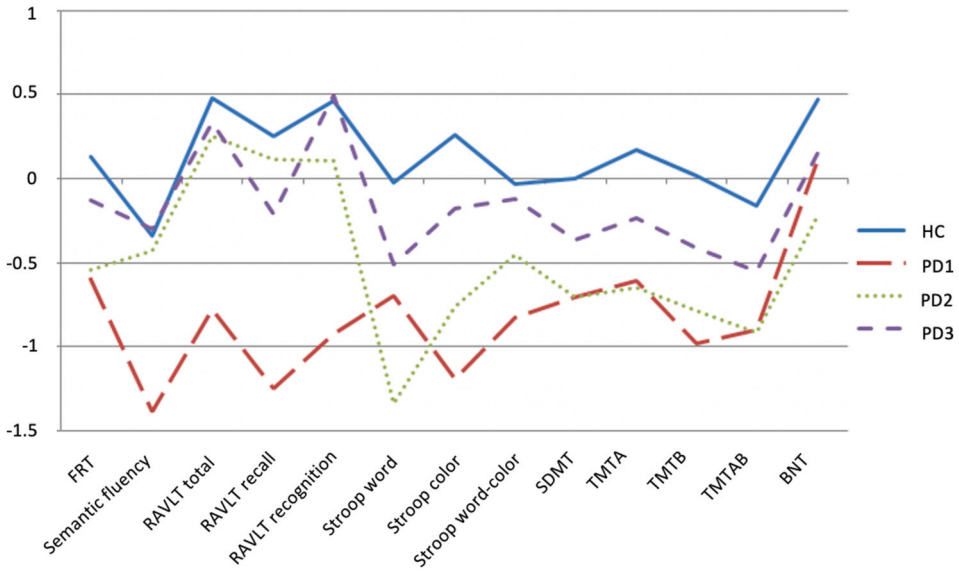

Fig. 3. Three-cluster solution – neuropsychological profiles. Neuropsychological profiles for healthy controls (blue), PD1 (red), PD2 (green) and PD3 (purple). Data are presented as z scores. The signs of TMTA, TMTB and TMTAB scores are flipped. In all cases, lower z scores indicate worse performance. Abbreviations: BNT – Boston Naming Test; FRT – Facial Recognition Test; HC – healthy controls; PD1 – Parkinson's disease patient subgroup 1; PD2 – Parkinson's disease patient subgroup 2; PD3 – Parkinson's disease patient group 3; RAVLT – Rey Auditory Verbal Learning Test; SDMT – Symbol Digits Modalities Test; Stroop color – Stroop color test; Stroop word – Stroop word test; Stroop word-color – Stroop word-color interference; TMTA – Trail Making Test Part A; TMTB – Trail Making Test Part B; TMTAB – Trail Making Test A minus B. Tests displayed are the ones showing significant differences between groups. (For interpretation of the references to color in this figure legend, the reader is referred to the Web version of this article.)

of different PD subtypes could help to elucidate previous controversial results on the study of WM abnormalities.

Our results suggest that only a subgroup with widespread GM atrophy showed WM alterations compared to HC, in line with the recent results of Abassi et al. [10] showing structural connectivity differences in PD subtypes. Unfortunately, in that study the authors did not report whole-brain FA differences in PD subtypes since the analyses were limited to the basal ganglia. Our results suggest that DTI abnormalities in PD patients could be understood as secondary to axonal degeneration after cortical and subcortical neuronal body damage, which consequently would be expected to be found alongside GM atrophy.

Our findings also revealed the existence of a third subgroup (PD3), which was the youngest group with earlier disease onset. Despite the similarity in other clinical variables between groups, PD3 patients did not show significant structural differences with HC neither in GM nor in WM, after controlling for age. Similarly, previous studies reported negative results when comparing PD patients without cognitive impairment and HC in cortical and subcortical GM using whole-brain VBM or WM methods [7,9]. Previous cortical thickness analyses also showed negative results when comparing PD and HC [21,22] or described differences that did not survive correction for multiple comparisons [23].

Regarding the neuropsychological performance of the PD subgroups, both PD1 and PD2 subtypes performed worse than HC in the Facial Recognition Test, TMT Part A and Part B, and Stroop Color Test; whereas PD3 performed similarly to HC. Moreover, PD1 also performed significantly worse than HC and PD3 in RAVLT and the semantic fluency test. It is noteworthy that the impairment in total learning and delayed recall verbal tasks characteristic of the PD1 subtype has been associated with future cognitive impairment in PD [24], the hippocampus being a key structure to understanding the memory changes in PD without dementia [25]. Additionally, PD1 had semantic memory impairment that agrees with the involvement of posterior cortical regions [4,26]. Specifically, posterior based cortical deficits, and semantic fluency in particular, have been shown to be a predictor of dementia in PD [27]. More precisely, the PD1 atrophy pattern also included the primary occipital cortex, just as it has been found before in early PD patients [28], and might be related to color perception deficits described in PD [29].

On the other hand, the PD2 subgroup did not show a detectable cognitive profile to distinguish it from other PD subgroups; however, the brain atrophy pattern in this group was clearly different. Despite a discreet overlap between PD1 and PD2, there is a dissociation between these groups: while the PD2 pattern consisted of a more prominent orbitofrontal atrophy including bilateral frontal medial regions, but also anterior areas, PD1 was characterized by extensive atrophic changes in bilateral temporo-parieto-occipital regions. This dissociation may have not only important cognitive but also behavioral and mood consequences. In this context, depression in PD has been related to decreased GM volume in orbitofrontal and temporal regions [30]. In the same way, apathy and recognition of emotions have been seen to correlate with GM volumes in the orbitofrontal cortex [31,32], the amygdala [31] and the temporal cortex [32]. Although we did not find significant differences between groups in BDI or the apathy scale, PD1 and PD2 yielded the highest percentage of subjects with apathy (close to 50%), while PD3 and HC showed lower percentages. In this regard, the inclusion of tests sensitive to orbitofrontal and posterior deficits in the neuropsychological batteries used to assess PD patients is of crucial interest as previously stated [3].

The need to better understand the heterogeneity seen in other neurodegenerative disorders, such as Alzheimer's disease (AD), has similarly led to the use of neuroimaging data and cluster analysis to assess the presence of potential subgroups [33]. Taking one step further, Jeon and colleagues recently used a multimodal cluster analysis based on cortical thickness, tau and amyloid depositions, which led to the characterization of three AD subgroups [34], mainly driven by the tau deposition and cortical atrophic pattern. However, multidimensionality remains a limitation of these studies, as well as of our work, despite our having managed to improve the high dimensionality problem compared with previous cluster analyses [3,34] through the use of only 85 features. Further progress in this issue will allow, for example, combining different diffusion measures in an optimal model in order to better characterize WM differences between PD subtypes. Another limitation would be that PD patients with a Hoehn and Yahr scale score above 3 were excluded from the study, which could have reduced the variability of the PD sample and, consequently, the probability of finding other PD groups. Finally, the wide confidence intervals of the neuropsychological data suggest that a larger sample would be required in order to more precisely identify cognitive differences between groups.

In conclusion, the use of unsupervised machine learning methods based on multimodal MRI data allows the classification of PD patients into the following subtypes: one group with cortical and subcortical GM atrophy, widespread WM abnormalities and worse cognition; a second group with mainly orbitofrontal and temporal cortical atrophy; and a third group without detectable GM or WM abnormalities, earlier disease onset and normal cognition. It is also worth noting that even though both WM and GM contributed to defining the different groups, GM

degeneration patterns were more relevant in the characterization of PD groups than WM alterations. Nevertheless, incorporating FA measures to the clustering algorithm implies moving one step closer to multimodal approaches. Moreover, these results add to recent evidence regarding different phenotypes in PD, which not only differ in cognitive performance but also in patterns of brain degeneration, thus lending further support to the hypothesis of distinct disease courses.

Appendix A. Supplementary data

Supplementary data to this article can be found online at https://doi.org/10.1016/j.parkreldis.2020.11.010.

Disclosures

This study was sponsored by the Spanish Ministry of Economy and Competitiveness (PSI2013-41393-P; PSI2017-86930-P cofinanced by Agencia Estatal de Investigación (AEI) and the European Regional Development Fund), by Generalitat de Catalunya (2017SGR748), Fundació La Marató de TV3 in Spain (20142310), and supported by María de Maeztu Unit of Excellence (Institute of Neurosciences, University of Barcelona) MDM-2017-0729, Ministry of Science, Innovation and Universities. AI and AC were supported by APIF predoctoral fellowship from the University of Barcelona (2017–2018). AA was supported by a fellowship from 2016, Departament d'Empresa i Coneixement de la Generalitat de Catalunya, AGAUR (2016FI_B00360). CU was supported by a fellowship from 2014, Spanish Ministry of Economy and Competitiveness (BES-2014-068173) and co-financed by the European Social Fund (ESF).

MJM received honoraria for advice and lecture from Abbvie, Bial and Merzt Pharma and grants from Michael J. Fox Foundation for Parkinson Disease (MJFF): MJF_PPMI_10_001, PI044024.

YC has received funding in the past five years from FIS/FEDER, H2020 programme, Union Chimique Belge (UCB pharma), Teva, Medtronic, Abbvie, Novartis, Merz, Piramal Imaging, and Esteve, Bial, and Zambon. YC is currently an associate editor for Parkinsonism and Related Disorders.

We are also indebted to the Magnetic Resonance Imaging core facility of the IDIBAPS for technical support (project IBPS15-EE-3688 cofunded by MCIU and by ERDF); and we acknowledge the CERCA Programme/Generalitat de Catalunya. We are especially grateful to all the participants in the study for their goodwill and generosity.

References

[1] K.R. Chaudhuri, G.G. Healy, A.H.V. Schapita, Non-motor symptoms of Parkinson's disease: diagnosis and management, Lancet Neurol. 5 (2006) 235–245. http://neurology.thelancet.com.

[2] L.V. Kalia, A.E. Lang, Parkinson's disease, Lancet 386 (2015) 896–912, https://doi.org/10.1016/S0140-6736(14)61393-3.

[3] C. Uribe, B. Segura, H.C. Baggio, A. Abos, M.J. Marti, F. Valldeoriola, et al., Patterns of cortical thinning in nondemented Parkinson's disease patients, Mov. Disord. 31 (2016) 699–708, https://doi.org/10.1002/mds.26590.

[4] C. Uribe, B. Segura, H.C. Baggio, A. Abos, A.I. Garcia-Diaz, A. Campabadal, et al., Progression of Parkinson's disease patients' subtypes based on cortical thinning: 4-year follow-up, Park. Relat. Disord. 64 (2019) 286–292, https://doi.org/10.1016/j.parkreldis.2019.05.012.

[5] N. Ibarretxe-Bilbao, E. Tolosa, C. Junque, M.J. Marti, MRI and cognitive impairment in Parkinson's disease, Mov. Disord. 24 (2009), https://doi.org/10.1002/mds.22670.

[6] C. Atkinson-Clement, S. Pinto, A. Eusebio, O. Coulon, Diffusion tensor imaging in Parkinson's disease: review and meta-analysis, NeuroImage Clin 16 (2017) 98–110, https://doi.org/10.1016/j.nicl.2017.07.011.

[7] T. Hattori, S. Orimo, S. Aoki, K. Ito, O. Abe, A. Amano, et al., Cognitive status correlates with white matter alteration in Parkinson's disease, Hum. Brain Mapp. 33 (2012) 727–739, https://doi.org/10.1002/hbm.21245.

[8] T.R. Melzer, R. Watts, M.R. MacAskill, T.L. Pitcher, L. Livingston, R.J. Keenan, J. C. Dalrymple-Alford, T.J. Anderson, White matter microstructure deteriorates across cognitive stages in Parkinson disease, Neurology 80 (2013) 1841–1849.

[9] F. Agosta, E. Canu, E. Stefanova, L. Sarro, A. Tomić, V. Špica, et al., Mild cognitive impairment in Parkinson's disease is associated with a distributed pattern of brain white matter damage, Hum. Brain Mapp. 35 (2014) 1921–1929, https://doi.org/10.1002/hbm.22302.

[10] N. Abbasi, S.M. Fereshtehnejad, Y. Zeighami, K.M.H. Larcher, R.B. Postuma, A. Dagher, Predicting severity and prognosis in Parkinson's disease from brain microstructure and connectivity, NeuroImage Clin 25 (2020), https://doi.org/10.1016/j.nicl.2019.102111.

[11] C.L. Tomlinson, R. Stowe, S. Patel, C. Rick, R. Gray, C.E. Clarke, Systematic review of levodopa dose equivalency reporting in Parkinson's disease, Mov. Disord. 25 (2010) 2649–2653, https://doi.org/10.1002/mds.23429.

[12] I. Litvan, J.G. Goldman, A.I. Tröster, B.A. Schmand, D. Weintraub, R.C. Petersen, et al., Diagnostic criteria for mild cognitive impairment in Parkinson's disease: Movement Disorder Society Task Force guidelines, Mov. Disord. 27 (2012) 349–356, https://doi.org/10.1002/mds.24893.

[13] D. Aarsland, K. Brønnick, J.P. Larsen, O.B. Tysnes, G. Alves, Cognitive impairment in incident, untreated Parkinson disease: the Norwegian ParkWest study, Neurology 72 (2009) 1121–1126, https://doi.org/10.1212/01.wnl.0000338632.00552.cb.

[14] G. Douaud, S. Smith, M. Jenkinson, T. Behrens, H. Johansen-Berg, J. Vickers, et al., Anatomically related grey and white matter abnormalities in adolescent-onset schizophrenia, Brain 130 (2007) 2375–2386, https://doi.org/10.1093/brain/awm184.

[15] S.M. Smith, M. Jenkinson, H. Johansen-Berg, D. Rueckert, T.E. Nichols, C. E. Mackay, et al., Tract-based spatial statistics: voxelwise analysis of multi-subject diffusion data, Neuroimage 31 (2006) 1487–1505, https://doi.org/10.1016/j.neuroimage.2006.02.024.

[16] M. Jenkinson, C.F. Beckmann, T.E.J. Behrens, M.W. Woolrich, S.M. Smith, Review FSL, Neuroimage 62 (2012) 782–790, https://doi.org/10.1016/j.neuroimage.2011.09.015.

[17] S. Wakana, A. Caprihan, M.M. Panzenboeck, J.H. Fallon, M. Perry, R.L. Gollub, K. Hua, J. Zhang, H. Jiang, P. Dubey, A. Blitz, P. van Zijl, S. Mori, Reproducibility of quantitative tractography methods applied to cerebral white matter, NeuroImage 36 (2007) 630–644, https://doi.org/10.1016/j.neuroimage.2007.02.049.

[18] A.M. Winkler, G.R. Ridgway, M.A. Webster, S.M. Smith, T.E. Nichols, Permutation inference for the general linear model, Neuroimage 92 (2014) 381–397, https://doi.org/10.1016/j.neuroimage.2014.01.060.

[19] S.M. Fereshtehnejad, Y. Zeighami, A. Dagher, R.B. Postuma, Clinical criteria for subtyping Parkinson's disease: biomarkers and longitudinal progression, Brain 140 (2017) 1959–1976, https://doi.org/10.1093/brain/awx118.

[20] F.X. Chen, D.Z. Kang, F.Y. Chen, Y. Liu, G. Wu, X. Li, et al., Gray matter atrophy associated with mild cognitive impairment in Parkinson's disease, Neurosci. Lett. 617 (2016) 160–165, https://doi.org/10.1016/j.neulet.2015.12.055.

[21] J.B. Pereira, D. Weintraub, K. Brønnick, A. Lebedev, E. Westman, D. Aarsland, Initial Cognitive Decline is Associated with Cortical Thinning in Early Parkinson Disease 82 (2014) 2017–2025. http://surfer.nmr.mgh.harvard.edu/fswiki, 2014.

[22] E. Mak, L. Su, G.B. Williams, M.J. Firbank, R.A. Lawson, A.J. Yarnall, et al., Baseline and longitudinal grey matter changes in newly diagnosed Parkinson's disease: ICICLE-PD study, Brain 138 (2015) 2974–2986, https://doi.org/10.1093/brain/awv211.

[23] J. Pagonabarraga, I. Corcuera-Solano, Y. Vives-Gilabert, G. Llebaria, C. García-Sánchez, B. Pascual-Sedano, et al., Pattern of regional cortical thinning associated with cognitive deterioration in Parkinson's disease, PloS One 8 (2013), e54980, https://doi.org/10.1371/journal.pone.0054980.

[24] G. Levy, D.M. Jacobs, M.X. Tang, L.J. Côté, E.D. Louis, B. Alfaro, et al., Memory and executive function impairment predict dementia in Parkinson's disease, Mov. Disord. 17 (2002) 1221–1226, https://doi.org/10.1002/mds.10280.

[25] C. Uribe, B. Segura, H.C. Baggio, A. Campabadal, A. Abos, Y. Compta, et al., Differential progression of regional hippocampal atrophy in aging and Parkinson's disease, Front. Aging Neurosci. 10 (2018) 1–9, https://doi.org/10.3389/fnagi.2018.00325.

[26] B. Segura, H.C. Baggio, M.J. Marti, F. Valldeoriola, Y. Compta, A.I. Garcia-Diaz, et al., Cortical thinning associated with mild cognitive impairment in Parkinson's disease, Mov. Disord. 29 (2014) 1495–1503, https://doi.org/10.1002/mds.25982.

[27] C.H. Williams-Gray, T. Foltynie, C.E.G. Brayne, T.W. Robbins, R.A. Barker, Evolution of cognitive dysfunction in an incident Parkinson's disease cohort, Brain 130 (2007) 1787–1798, https://doi.org/10.1093/brain/awm111.

[28] C. Uribe, B. Segura, H.C. Baggio, A. Abos, A.I. Garcia-Diaz, A. Campabadal, et al., Cortical atrophy patterns in early Parkinson's disease patients using hierarchical cluster analysis, Park. Relat. Disord. 50 (2018) 3–9, https://doi.org/10.1016/j.parkreldis.2018.02.006.

[29] R.B. Postuma, J Gagnon, J Bertrand, D.G Marchand, J.Y. Montplaisir, Parkinson risk in idiopathic REM sleep behavior disorder: preparing for neuroprotective trials, Neurology 84 (11) (2015) 1104–1113, https://doi.org/10.1212/WNL.0000000000001364.

[30] A. Feldmann, Z. Illes, P. Kosztolanyi, E. Illes, A. Mike, F. Kover, et al., Morphometric changes of gray matter in Parkinson's disease with depression: a voxel-based morphometry study, Mov. Disord. 23 (2008) 42–46, https://doi.org/10.1002/mds.21765.

[31] N. Ibarretxe-Bilbao, C. Junque, E. Tolosa, M.J. Marti, F. Valldeoriola, N. Bargallo, et al., Neuroanatomical correlates of impaired decision-making and facial emotion recognition in early Parkinson's disease, Eur. J. Neurosci. 30 (2009) 1162–1171, https://doi.org/10.1111/j.1460-9568.2009.06892.x.

[32] H. Alzahrani, A. Antonini, A. Venneri, Apathy in mild Parkinson's disease: neuropsychological and neuroimaging evidence, J. Parkinsons Dis. 6 (2016) 821–832, https://doi.org/10.3233/JPD-160809.
[33] Y. Noh, S. Jeon, J.M. Lee, S.W. Seo, G.H. Kim, H. Cho, et al., Anatomical heterogeneity of Alzheimer disease Based on cortical thickness on MRIs, Neurology 83 (2014) 1936–1944, https://doi.org/10.1212/WNL.0000000000001003.
[34] S. Jeon, J.M. Kang, S. Seo, H.J. Jeong, T. Funck, S.Y. Lee, et al., Topographical heterogeneity of Alzheimer's disease based on MR imaging, tau PET, and amyloid PET, Front. Aging Neurosci. 10 (2019) 1–10, https://doi.org/10.3389/fnagi.2019.00211.